SCIENTIFIC PROBLEMS
OF MACHINES OPERATION
AND MAINTENANCE
4 (168) 2011

RYSZARD SZCZEPANIK[*], EDWARD ROKICKI [*],
JAROSŁAW SPYCHAŁA[*], ROMUALD RZADKOWSKI[**]

Reliability of middle bearing in SO-3 jet engine

Key words

Reliability of bearing, pick detector, technical condition of jet engine bearings, blade tip-timing.

Słowa kluczowe

Niezawodność łożyska, detektor szczytowy, stan techniczny łożysk silnika odrzutowego, czas przyjścia łopatki.

Summary

In the last years damages of the middle bearing of SO-3 engines were the reasons of serious air incidents. In this paper the pick detector analysis of tip-timing data has been applied as an alternative method of studying the results of experimental research. Measurements of seventh stage compressor rotor blade vibrations were made using the tip-timing method at the AFIT. The experimental analyses concerned both an SO-3 engine with a middle bearing in a good technical condition and an engine with a damaged middle bearing. A numerical analysis of the free vibration of the seventh stage blade was conducted to verify the experimental ones. The seventh compressor rotor blade of an SO-3 engine (close to the middle bearing) was modelled using an FE model and its natural frequencies were calculated. The method presented in this paper enables prediction of middle bearing failure in an SO-3 engine 33 minutes before it happens.

[*] Air Force Institute of Technology, Księcia Bolesława Street 6, 01-494 Warsaw, Poland.
[**] Institute of Fluid-Flow Machinery, Polish Academy of Sciences, Gen. J. Fiszera Street 14, 80-952 Gdańsk, Poland.

Introduction

Rolling element bearings are one of the most essential parts in rotating machinery. During operation, bearings are often subjected to high loading and difficult working conditions, which in turn often lead to the development of defects in the bearing components [1]. One way to increase operational reliability is to monitor incipient faults in these bearings [2–4]. Analytical models for predicting the vibration frequencies of rolling bearings and the amplitudes of significant frequencies with localised defects in bearings have been proposed in [5], [6], and [7].

FFT is one of the widely used fault detection techniques [8], [9]**.** The only drawback of FFT based methods is that they are not suitable for non-stationary signals. In recent years, a new time frequency analysis technique, called Wavelet Analysis, was developed. The advantage of Wavelet Analysis is that the non-stationary characteristic of a signal can be easily highlighted in its spectrum [8], [9], [10], [11], and [12].

The tip-timing technique is generally used for diagnosing rotor blade displacements during rotation with a wide range of speeds [13, 14]. In this paper, the tip-timing technique is used for diagnosing displacements of seventh-stage compressor rotor blades and the middle bearing close to this stage. Such an analysis is important, because the failure of the middle bearing of an SO-3 was reported in 1993 [13], [14] (Figs. 1, 2). This paper proposes the first methodology to predict such failures.

Measurements of seventh-stage compressor rotor blades vibrations were made using the tip-timing method at the Air Force Institute of Technology in Warsaw. In order to understand better the experimental results, numerical calculations were also conducted for seventh-stage compressor rotor blades using the FE method.

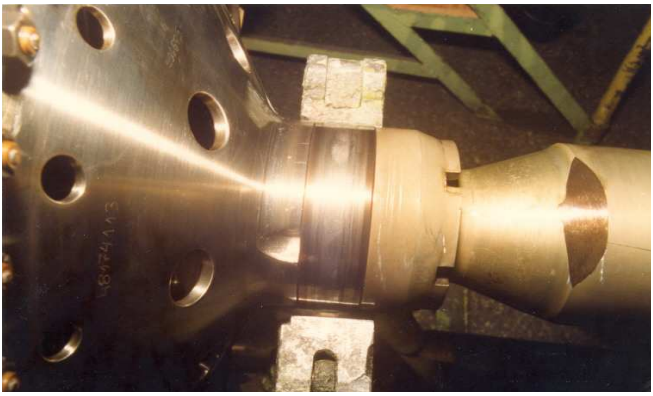

Fig. 1. The inner running track of the SO-3 engine middle bearing
Rys. 1. Bieżnia wewnętrzna łożyska środkowego silnika typu SO-3

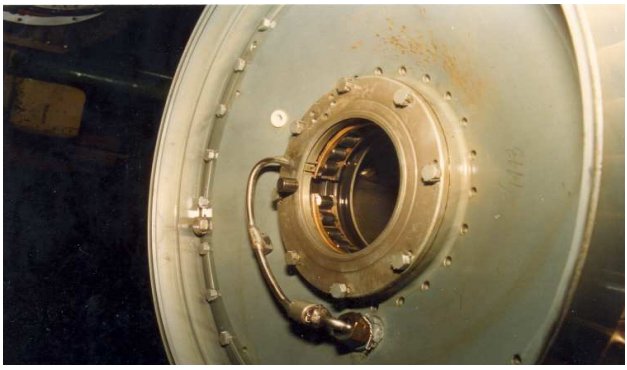

Fig. 2. Damaged elements of the SO-3 engine middle bearing
Rys. 2. Uszkodzone elementy łożyska środkowego silnika typu SO-3

Numerical results

The seventh-stage rotor blades of an SO-3 engine (close to the middle bearing) was modelled using an FE model, and its natural frequencies were calculated (table 1). The number of natural frequencies is presented in the first column. The second and fourth columns show the calculated natural frequencies for a non-rotating blade and one rotating at 15000 rpm, respectively. The third column presents the natural frequencies obtained experimentally. In real compressors, every rotor blade is different, so the natural frequencies of each rotor blade also differ. For example, in our experiment, the natural frequencies of seventh-stage rotor blades in the first mode ranged from 1620 Hz to 1932 Hz.

Table 1. Measured and numerically calculated natural frequencies of a seventh-stage rotor blade
Tabela 1. Zmierzone i wyliczone numerycznie częstotliwości drgań własnych łopatek siódmego stopnia wirnika

Mode number	Calculated 0 rpm	Experiment 0 rpm	Calculated 15000 rpm
	[Hz]	[Hz]	[Hz]
1	1765.2	<1620, 1932>	1921.6
2	4913.2	<4592, 5104>	4962.4
3	8247.0	<7920, 8272>	8376.1
4	12621	<12064, 12256>	12697
5	13867	-	13903
6	15360		15383
7	20973		21084
8	23368		23440
9	25174		25289
10	30445		30457

A comparison between the numerical and experimental results (made for stationary blades) was satisfactory. For example, the first calculated frequency was 1765.2 Hz, whereas in the experiment it was <1620, 1930> Hz. Measurements were made only up to the fourth blade mode. Fig. 3 presents a Campbell diagram for the rotor blade [17], which shows that 7EO, 8EO, and 9EO can cause higher rotor blade responses.

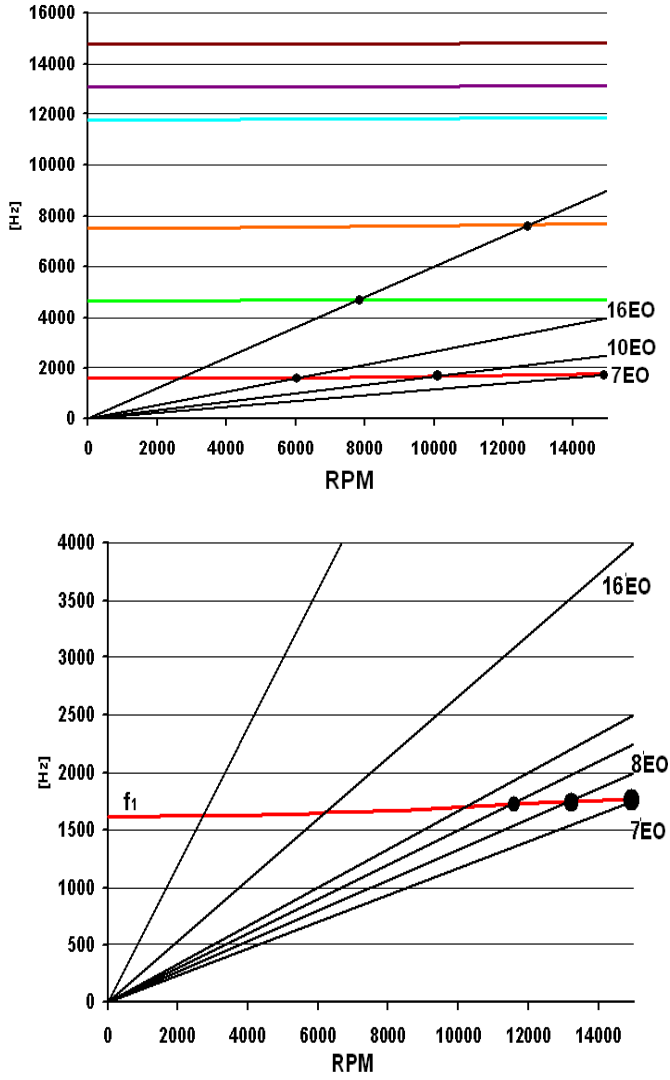

Fig. 3. Campbell diagram of the seventh-stage compressor rotor blade of an SO-3 engine
Rys. 3. Wykres Campbell'a łopatek siódmego stopnia wirnika sprężarki silnika typu SO-3

Experimental results

The tip-timing measurement of seventh-stage compressor rotor blades is presented in Fig. 4. This stage consisted of 48 rotor blades. This graph shows displacements of each of the 48 rotor blades at rotation speeds ranging from 7000 rpm to 15500 rpm. As can be seen, 7EO and 8EO create greater rotor blade responses. Each blade responded at a different time (see circled regions in Fig. 4). Tip-timing is a non-contact measurement technique which uses probes mounted in the casing to determine the vibration of all of the blades. The results for individual blades could not explain the bearing failure, and for this reason the peak detector method was applied. The entire test run time was divided into short periods: T. An average amplitude of all the seventh-stage blades (RMS) was calculated for each T period [19]:

$$RMS(t) = \left(\frac{1}{T} \int_0^T r_w^2(t)\, dt \right)^{\frac{1}{2}} \tag{1}$$

where $r_w(t)$ is the measured signal in period T.

A DIL1 filter was used to measure the vibration signal of the rotor blades from 0.1 Hz to 1000 Hz.

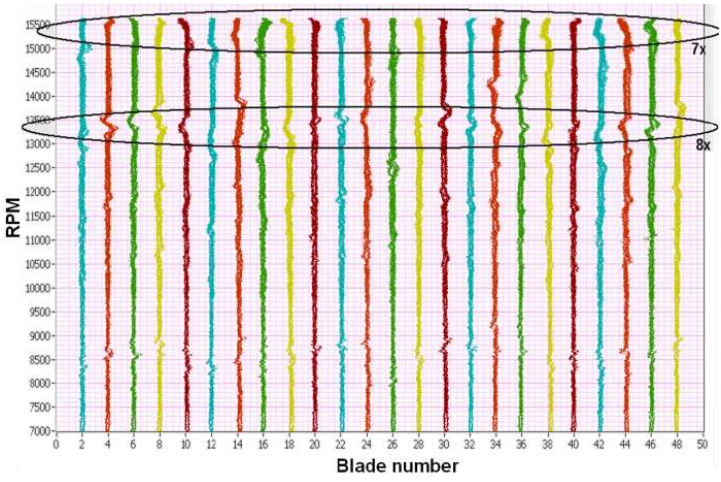

Fig. 4. The tip-timing measurement of the seventh-stage compressor rotor blades of SO-3 engine [16]
Rys. 4. Wykres drgań łopatek siódmego stopnia wirnika sprężarki silnika typu SO-3 wyznaczony metodą „tip-timing” [16]

Fig. 5 presents the RMS displacements value of seventh-stage rotor blades (Eq. (1)) for an assumed test run (the plane x-y, RPM versus time) with the middle bearing working properly. The rotor blade amplitude for 7EO was close to the nominal speed (see Campbell diagram Fig. 3). In order of magnitude, the next resonances appeared at 12000 rpm and were excited by 8EO (see Campbell diagram). There were some other resonances whose origins were difficult to explain using the Campbell diagram of a rotor blade of the seventh-stage compressor. The maximal value of RMS amplitude of rotor blades was equal to 7e-5 m.

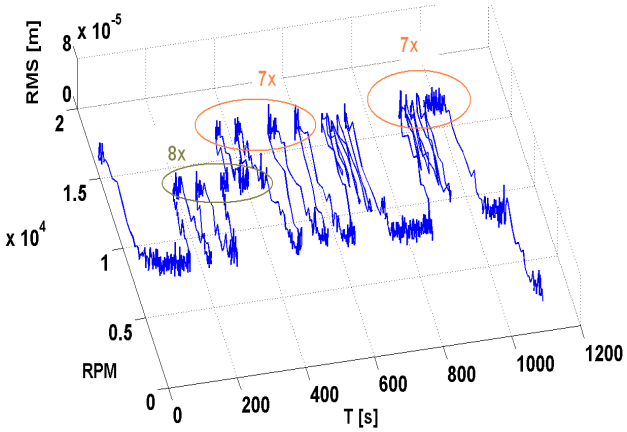

Fig. 5. The measured vibration amplitude RMS of the seventh-stage compressor rotor blade with the middle bearing working properly [18]
Rys. 5. Zmierzona amplituda RMS drgań łopatek siódmego stopnia wirnika sprężarki z łożyskiem pracującym poprawnie [18]

Experiments were carried out at the Air Force Institute of Technology in Warsaw to find out when a partly damaged middle bearing would fail in an SO-3 engine.

A peak detector analysis provided an alternative method for studying the experimental results. This analysis is based on calculating new averaged blade amplitudes RMSn in periods T according to the following equation [19]:

$$\mathrm{RMSn}(t+\Delta t) = \mathrm{RMSn}(t)\left(\frac{\tau-1}{\tau}\right) + \frac{\mathrm{RMS}(t+\Delta t)}{\tau} \tag{2}$$

if RMS (t) > RMSn (t) then $\tau = 400$,
RMS (t) < RMSn(t) then $\tau = 2000$,

with RMS (t) taken from Eq (1).

Fig. 6, for instance, presents the averaged blade amplitudes RMSn (red) obtained from the measured blade vibration RMS signal (blue). Equation 2 presents a blade signal averaging formula that reduces the peaks and increases the minimal values. The objective of this formula is to obtain an average vibration amplitude at any given time period. If an engine is damaged, this averaged amplitude will rise.

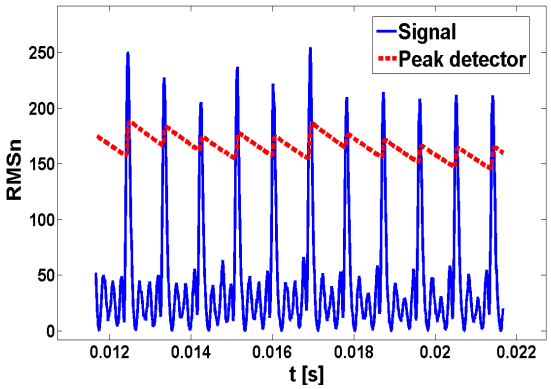

Fig. 6. The peak detector results for measurement signal
Rys. 6. Wynik przetworzenia zmierzonego sygnału po zastosowania detektora szczytowego

The peak detector was used for an SO-3 engine with a sensor placed in the casing above the seventh compressor stage. The blue line in Fig.7 represents the run test. RPM (rotations per minute) was normalised to RPMn in order to fit the curve RMSn, which changes from 0.81 to 1.1. The red dashed line represents the RMSn values of (Eq. (2)). The values of RMSn start from 1, for a cold engine, and decrease with time to values below 1. This means that when a cold engine is run-up, the vibration amplitude first increases and then decreases. In our case, the amplitude reached the level of a normally working engine after 180 s. The RMSn signal changed by no more than 20% throughout the test.

A peak detector analysis Eq. (2) was also conducted in the case of bearing failure (see Fig. 8). The blue line in Fig. 8 is the run test (RPMn), while the red dashed line represents the RMSn (Eq. (2)). The damaged bearing caused increasing vibration amplitude fluctuations. The level of RMSn amplitude increased to 1.62 (Fig. 8); whereas, in the engine with a normally working middle bearing, it only increased to 0.9 (Fig. 7). The calculated signal variations reached 70% and were a symptom of increasing bearing failure, although the engine was still working. As mentioned above, in the case of the undamaged bearing, the RMSn varied by no more than 20%. Figure 8 presents the first stage of the experiment, where vibration amplitude measurements were completed before the middle bearing was permanently damaged.

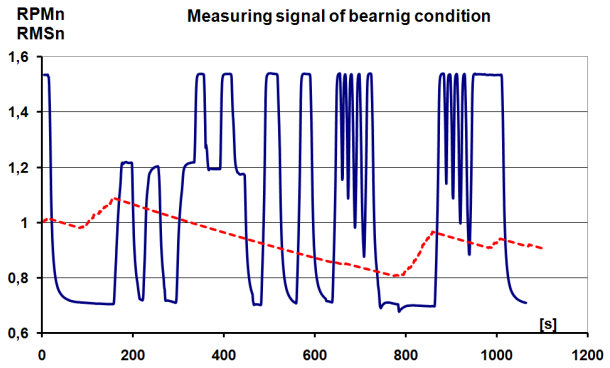

Fig. 7. Peak detector amplitude (RMSn) of SO-3 engine seventh-stage compressor rotor blade without damaged middle bearing
Rys. 7. Amplituda (RMSn) detektora szczytowego dla łopatek siódmego stopnia wirnika sprężarki silnika typu SO-3 bez uszkodzenia łożyska

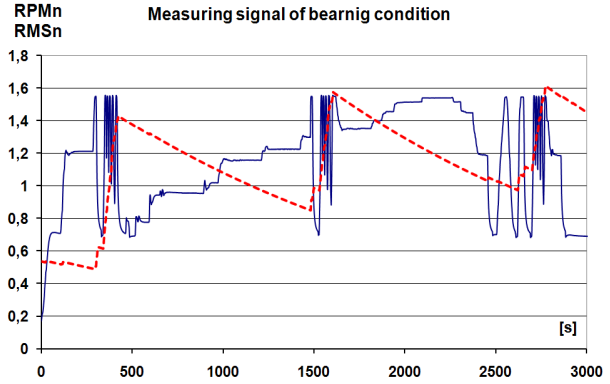

Fig. 8. The peak detector amplitude (RMSn) of seventh-stage compressor rotor blade of SO-3 engine – experiment with the damaged bearing
Rys. 8. Amplituda (RMSn) detektora szczytowego dla łopatek siódmego stopnia wirnika sprężarki silnika typu SO-3 – eksperyment z uszkodzonym łożyskiem

Fig. 9 presents the RMS displacements value of seventh-stage rotor blades (Eq. (1)) for an assumed test run (the plane x-y, RPM versus time) in the case of bearing failure. The maximal rotor blade amplitude for 7EO was close to the nominal speed (see Campbell diagram Fig. 3). There were some other resonances whose origins were difficult to explain using the Campbell diagram of a rotor blade of the seventh-stage compressor. The maximal value of RMS amplitude of rotor blades was equal to 7e-4 m.

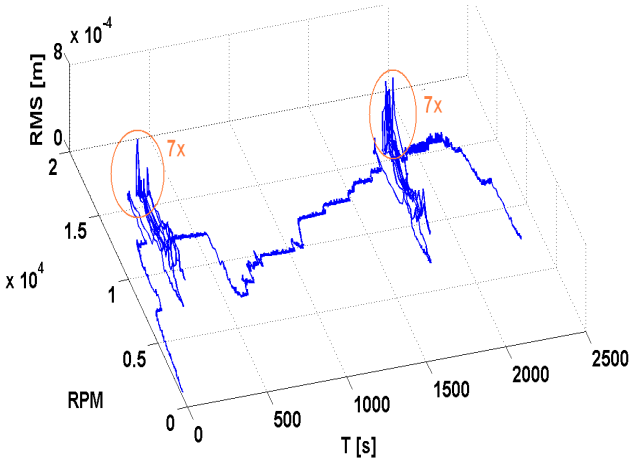

Fig. 9. The measured vibration amplitude RMS of the seventh-stage compressor rotor blade in the case of bearing failure
Rys. 9. Zmierzona amplituda RMS drgań łopatek siódmego stopnia wirnika sprężarki w przypadku uszkodzenia łożyska

Next, a new test run was started (Fig. 10), in which, after 2000 s, bearing failure caused the seventh-stage rotor blades to rub against the casing and the engine had to be stopped. In this case, the RMSn value was almost 1.84.

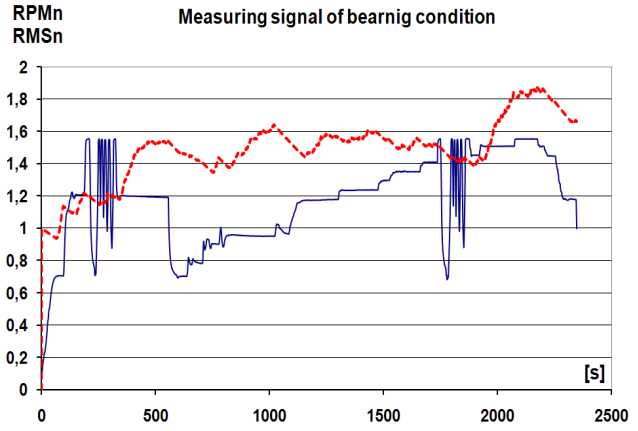

Fig. 10. Peak detector amplitude (RMSn) of seventh-stage compressor rotor blade vibration with fully damaged middle bearing
Rys. 10. Amplituda (RMSn) detektora szczytowego dla drgań łopatek siódmego stopnia wirnika sprężarki z całkowicie uszkodzonym łożyskiem środkowym

Fig. 11 presents the RMS displacement value of seventh-stage rotor blades (Eq. (1)) for an assumed test run (the plane x-y, RPM versus time) with a fully damaged middle bearing. The maximal rotor blade amplitude for 7EO was close to the nominal speed (see Campbell diagram Fig. 3). There were some other resonances whose origins were difficult to explain using the Campbell diagram of a rotor blade of the seventh-stage compressor. The maximal value of RMS amplitude of rotor blades was equal to 2e-3 m.

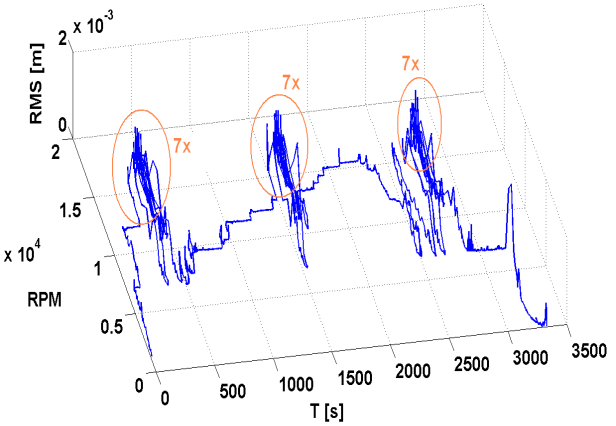

Fig. 11. The measured vibration amplitude RMS of the seventh-stage compressor rotor blade with fully damaged middle bearing
Rys. 11. Zmierzona amplituda RMS drgań łopatek siódmego stopnia wirnika sprężarki z całkowicie uszkodzonym łożyskiem środkowym

Conclusions

Failure of the middle bearing in an SO-3 engine was reported. A tip-timing analysis of the (seventh-stage compressor) rotor blades above the middle bearing was carried out. Next, a numerical analysis of the free vibration of a seventh-stage blade was conducted to verify the experimental results. A peak detector analysis was also conducted, using the same sensors as the ones used in the tip-timing analysis. The experimental analyses were carried out on an SO-3 engine with an undamaged middle bearing and then with a damaged middle bearing.

The method presented in this paper enables the prediction of middle bearing failure in an SO-3 engine 33 minutes before it happens.

Acknowledgment

This research has been financed by Polish Government funds for the years 2009 to 2012 as a development project 0R00010209. All numerical calculations were made at the Academic Computer Centre TASK (Gdańsk, Poland).

References

[1] Zhang B., Georgoulas G., Orchard M., Saxena A., Brown D., Vachtsevanos G. and Liang S, (2008), Rolling Element Bearing Feature Extraction and Anomaly Detection *VETOMAC–VI I. Angello, S.K. Khuntia and A. Chatterjee* 366 Based on Vibration Monitoring, 16th Mediterranean Conference on Control and Automation Congress Centre, Ajaccio, France, June 25–27.

[2] Monavar H.M, Ahmadi H.and Mohtasebi S.S, (2008), Prediction of defects in roller bearings using vibration signal analysis, World Applied Sciences Journal, Vol. 4(1), pp. 150–154.

[3] Yang H., Mathew J. and Ma J., (2005), Fault diagnosis of rolling element bearings using basis pursuit, Mechanical Systems and Signal Processing, Vol. 19, pp. 341–356.

[4] McInerny S. A. and Dai Y, (2003), Basic vibration signal Processing for Bearing Fault Detection, IEEE transactions on education, Vol. 46(1), pp. 149.

[5] Tandon N. and Choudhury A, (1997), An analytical model for the prediction of the vibration response of rolling element bearings due to a localized defect, J. Sound and Vib, Vol. 205(3), pp. 275–292.

[6] Mc Fadden P.D. and Smith J.D., (1984), Model for the vibration produced by a single point defect in a rolling element bearing, J. Sound and Vib, Vol. 96(1), pp. 69–82.

[7] Mc Fadden P.D. and Smith J.D., (1985), The vibration produced by multiple point defects in a rolling element bearing, J. Sound and Vib, Vol. 98(2), pp. 263–273.

[8] Rao J.S. Vibratory Condition Monitoring of Machines, narosa Publishing House, 2000.

[9] Bari H.M. Bearing and Fan Failure Diagnostic Using Vibratory monitoring: A Sase Study, Proceedings of the 6th International Conference on Vibration Engineering and Technology of Machinery, VETOMAC –VI, Ed. K.Gupta, S.P. Singh, J.K. Darpe, MACMILLAN, 876––886, 2010.

[10] Angello, I. and Chatterjee, A. , Extraction of Non Stationary Characteristics of Rolling Element Bearings for Fault Diagnosis Using Wavelet Analysis, Proceedings of International Conference on advances in mechanical engineering, 3–5 Aug 09, SVNIT-Surat, 497.

[11] Lin J. and Qu, L, (2000), Feature extraction based on Morlet wavelet and its application for mechanical fault diagnosis, J. Sound and Vib ,Vol. 234(1), pp. 135–148.

[12] Lin J.Z. and Fyfe K.R. (2004), Mechanical fault detection based on the wavelet de-noising technique, J. Vib. and Acoustics., Vo. 126, pp. 9–16.

[13] Nikolaou N.G. and Antoniadis I.A., (2002), Demodulation of vibration signals generated by defects in rolling element bearings using Complex Shifted Morlet Wavelets, Mechanical Systems and Signal Processing, Vol. 16(4), pp. 677–694.

[14] Szczepanik R., Witoś M., Szczepankowski A. and Bekiesiński R. Report 3/34/94 of failure reasons of the middle bearing of SO-3W engine. No 48173105", ITWL 10943/I, Warsaw, 1994.

[15] Kierszko Z. Report 1/34/95 of Engine Inspection SO-3 no 37177124. SO-3 no 37174264, SO-3W no 48174113, ITWL 11123/I, Warsaw, 1995.

[16] Przysowa R., The estimation of the technical state of aircraft engine rotor using digital method of converting the experimental signal from rotor blades. PhD Thesis. ITWL, 2007.

[17] Szczepanik R. Experimental analysis of rotor blades of aircraft engines in various operating conditions. Dsc Thesis, ITWL Warsaw, 2009.

[18] Rokicki E., Rządkowski R. and Szczepanik R. Experimental analysis of the first and seventh rotor blades of SO-3 compressor stage and turbine stage, IMP PAN, 263 /08, Gdańsk, 2008.

[19] Svan 948 - manual

Niezawodność łożyska środkowego silnika odrzutowego SO-3

S t r e s z c z e n i e

W ostatnich latach uszkodzenia środkowego łożyska silnika typu SO-3 były przyczynami poważnych zdarzeń lotniczych. W niniejszym artykule, jako alternatywna metoda do analizy danych uzyskanych metodą „tip-timing" podczas badań eksperymentalnych, został zastosowany detektor szczytowy. Pomiary drgań łopatek siódmego stopnia sprężarki zostały przeprowadzone z wykorzystaniem metody „tip-timing" w ITWL. Badania eksperymentalne dotyczyły zarówno silnika z łożyskiem środkowym o dobrym stanie technicznym, jak i łożyska uszkodzonego. W celu weryfikacji badań eksperymentalnych wykonano analizy numeryczne drgań własnych łopatek siódmego stopnia wirnika sprężarki. Łopatki tego stopnia, znajdującego się w strefie łożyska środkowego, zamodelowano, używając metody elementów skończonych, a następnie wyliczono ich częstotliwości drgań własnych. Metoda przedstawiona w artykule umożliwiła zidentyfikowanie symptomów uszkodzenia łożyska środkowego silnika SO-3 na 33 minuty przed awarią.